Dynamic light scattering measurements of azimuthal and zenithal anchoring of nematic liquid crystals

Mojca Vilfan,[1] Alenka Mertelj,[1] and Martin Čopič[1,2]
[1]*J. Stefan Institute, Jamova 39, SI-1000 Ljubljana, Slovenia*
[2]*Department of Physics, University of Ljubljana, Jadranska 19, SI-1000 Ljubljana, Slovenia*
(Received 27 June 2001; revised manuscript received 7 December 2001; published 8 April 2002)

Dynamic light scattering is used to obtain the anchoring energy coefficients of nematic liquid crystal (4-*n*-pentyl-4′-cyanobiphenyl) on rubbed nylon and photoactive poly-(vinyl-cinnamate). The anchoring coefficients are determined by measuring the relaxation time of the fundamental director fluctuation mode in a homogeneously aligned wedge cell as a function of cell thickness. The method is nonperturbative as no external torque is applied to the liquid crystal during the measurement. We show that by using two different scattering geometries, both azimuthal and zenithal anchoring energy coefficients can be measured on the same sample. The obtained zenithal anchoring coefficient is found to be, in contrast to previously reported results, approximately only two times larger than the azimuthal one. The effect of higher order fluctuation modes on the detected autocorrelation function is in good agreement with numerical calculations.

DOI: 10.1103/PhysRevE.65.041712 PACS number(s): 61.30.Hn, 78.35.+c

I. INTRODUCTION

Uniform and stable liquid crystal (LC) surface alignment is the basis for many applications of liquid crystals in industry. The alignment is achieved by depositing liquid crystal on a properly treated anisotropic alignment substrate that orients LC in a preferred direction (easy axis). The standard way of obtaining the required anisotropy of the substrate is mechanical rubbing of a polymer, usually polyimide or Nylon [1–3]. Such alignment is very stable and strong surface anchoring of liquid crystals is observed. The mechanism of the alignment, i.e., how the rubbing alters the surface and results in a uniformly oriented liquid crystal, is still not fully understood although many experiments including atomic force microscopy [4,5], x-ray spectroscopy [6,7], optical second-harmonic generation [8], and sum-frequency vibrational spectroscopy [9] were performed. The most probable seems the idea that the alignment is a consequence of the oriented state of the polymer chains [10]. Another method of liquid crystal alignment is oblique evaporation of silicon oxide on glass plates [11]. The method is interesting as the induced alignment can be either planar, homeotropic, or tilted, depending on the angle between the evaporation beam and the glass plate.

About a decade ago, Gibbons *et al.* [12] proposed a new alignment technique using photoactive substances that undergo selective isomerization or dimerization when illuminated by polarized light. This optical method of alignment is noncontact and, therefore, many drawbacks of buffing, such as the always present possibility of generating dust or electrostatic charge on the alignment layer, are avoided [13]. Also patterns and pixels with variations in the orientation of the director are easier to obtain by illumination than by rubbing. The anchoring on photoactive layers is much weaker than in the case of rubbed polymers and temporal instabilities in the alignment were observed [14,15]. Recently, a variety of other alignment techniques have emerged. Liquid crystals can be aligned on Langmuir-Blodgett films [16], on photopolymeric liquid crystals [17], or on self-assembled monolayers [18]. Ruetschi *et al.* [19] proposed liquid crystal alignment on surfaces treated with the tip of the atomic force microscope. The latest developments in the liquid crystal alignment include alignment with atomic beams [20].

A parameter that quantitatively describes the orientation-dependent anisotropic interactions between the liquid crystal molecules and the aligning substrate is the anchoring energy coefficient [21–23]. It is introduced as the torque per unit area, needed to turn the director away from the easy axis, divided by the angle of rotation. It is assumed that the deviations from the easy axis are small. Two different parameters are usually introduced: the azimuthal (in-plane) anchoring energy coefficient W_φ, corresponding to deviations from the easy axis in the LC-substrate plane, and zenithal (out-of-plane) anchoring coefficient W_ϑ, corresponding to deviations perpendicular to the substrate plane. The standard measurements of the anchoring energy coefficients observe the response of the LC sample to an applied external torque. The external field is either mechanical [24–26], electric [27–30], or magnetic [31–33]. The external field, however, induces a change in the configuration of the director in the sample and the director at the surface deviates from the easy axis. The measured anchoring strength can, therefore, depend on the thickness of the deformed layer as stated by Jérôme [23]. Moreover, it has been shown [34] that strong applied fields can result in melting of the liquid crystal rather than in a strong elastic deformation dictated by the external fields. Consequently, the anchoring energy coefficients measured by applying external torque can depend on the imposed deformation and on the field strength. The reported values of the azimuthal and zenithal anchoring coefficients show that zenithal anchoring is usually stronger than azimuthal and that there is one or even two orders of magnitude difference in the numerical values of these coefficients [23]. However, the two coefficients have never been obtained on a single sample, they were determined using different samples and different experimental methods.

We propose an alternative method for measuring the an-

choring energy coefficients by using dynamic light scattering [35–37] where no external torques act on the liquid crystal. The method is based on the observation of thermally excited orientational fluctuations in a thin undistorted sample. In bulk, the spectrum of fluctuations is continuous, with the relaxation rate at a given wave vector determined by the ratio of the corresponding elastic constant to viscosity. In a thin slab the components of the wave vector perpendicular to the slab are discrete. The relaxation rates of the modes, especially the lowest order ones, depend also on the boundary conditions, i.e., surface anchoring. As will be shown below, measurements of the lowest order relaxation rate as a function of the LC cell thickness enable us to determine also the anchoring strength. This approach was first used by Wittebrood *et al.* [38] who measured the fluctuation relaxation times in a liquid crystal between a flat surface and a glass lens. The authors determined the azimuthal anchoring energy coefficient in the case of weak anchoring and roughly estimated the zenithal anchoring strength in a hybrid sample. Using the same principle on a wedge cell [15,39], we studied the azimuthal anchoring coefficient on photoalignment layers.

In this paper we extend the dynamic light scattering method to measure both azimuthal and zenithal anchoring energy coefficients using the same nematic liquid crystal cell. The measurements were performed on different substrates in order to investigate different anchoring regimes, using rubbed nylon for strong anchoring and illuminated poly-(vinyl-cinnamate) PVCi for weak anchoring. The two anchoring regimes yield different dependencies of the relaxation time of the fundamental fluctuation mode on sample thickness, i.e., linear dependence for weak, and quadratic dependence for strong anchoring. The influence of the higher relaxation modes is also discussed. Both azimuthal and zenithal anchoring coefficients are determined on the same sample and it is found that the zenithal anchoring is stronger than the azimuthal, however, in contrast to previously reported results, only by a factor of 2.

II. ORIENTATIONAL FLUCTUATIONS IN THIN NEMATIC CELLS

Director fluctuations in a bulk nematic liquid crystal can be described by overdamped sinusoidal waves. In an unlimited sample two types of eigenmodes are present [36,40]: the first one being a combination of splay and bend elastic deformations (mode 1), and the second a combination of twist and bend deformations (mode 2). The relaxation time $\tau_i(\mathbf{q})$ $(i=1,2)$ of these eigenmodes is [40]

$$\frac{1}{\tau_i(\mathbf{q})}=\frac{K_i q_\perp^2+K_3 q_\parallel^2}{\eta}, \tag{1}$$

where K_i is splay (K_1) or twist (K_2) Frank elastic constant and K_3 is the bend elastic constant. The vector component $q_\perp$ is the fluctuation wave vector component perpendicular to the director $\mathbf{n_0}$, $q_\parallel$ is the component parallel to $\mathbf{n_0}$, and η is the effective rotational viscosity. In general, the director fluctuations $\delta\mathbf{n}$ that represent small deviations of the director from its equilibrium orientation $\mathbf{n_0}$ are given by the diffusion equation [40,41], for simplicity written in the one-constant approximation

$$K\nabla^2\delta\mathbf{n}=\eta\frac{\partial}{\partial t}\delta\mathbf{n}. \tag{2}$$

Let us now consider a thin planar sample of thickness d, which is confined in the z direction. The fluctuation dynamics is then determined by the boundary conditions [41]

$$W\delta\mathbf{n}\pm K\frac{\partial}{\partial z}\delta\mathbf{n}\bigg|_{z=0,d}=\mathbf{0}. \tag{3}$$

The solutions of Eq. (2) with the boundary conditions, given by Eq. (3), are the fluctuation eigenmodes in confined planar samples, which are overdamped standing waves in the z direction and undistorted waves in the directions parallel to the plates [41,42]. If the fluctuations with $q_\parallel=0$ are observed, the modes become pure splay and pure twist modes. The allowed fluctuation wave numbers q_z in the direction perpendicular to the glass plates, and to the director, are in thin samples discrete and for the even modes their values are given by the secular equation [41]

$$q_z\tan\left(q_z\frac{d}{2}\right)=\frac{W}{K}. \tag{4}$$

If the twist fluctuation mode, related to the fluctuations parallel to the LC-substrate interface, is observed, the corresponding elastic constant is the twist Frank elastic constant K_2 and the anchoring energy coefficient in Eq. (4) is W_φ. The secular equation [Eq. (4)] is valid also for the fluctuation wave vectors of the pure splay mode, where $\delta\mathbf{n}\|\mathbf{q}$. In this case, the corresponding constant is K_1 and the anchoring coefficient is W_ϑ.

Often the term extrapolation length [40] is introduced as the ratio of the elastic constant to the anchoring strength: $\lambda_\varphi=K_2/W_\varphi$ for azimuthal and $\lambda_\vartheta=K_1/W_\vartheta$ for zenithal anchoring. The extrapolation lengths indicate whether the anchoring in a sample is regarded as strong, when λ is smaller or comparable to the sample thickness d, or weak, when λ is much larger than d.

In the case of infinitely strong anchoring $(W\to\infty)$, the secular equation [Eq. (4)] can be exactly solved and the eigenvalues for the nth mode are given by

$$q_{zn}=\frac{(2n+1)\pi}{d}, \quad n=0,1,2,3,\ldots. \tag{5}$$

Taking into account Eq. (1), the fluctuation relaxation time of the fundamental mode $(n=0)$ for infinitely strong anchoring depends only on the sample thickness and viscoelastic constants of the liquid crystal,

$$\tau_0=\frac{\eta}{K}\frac{d^2}{\pi^2}. \tag{6}$$

If the anchoring is strong but finite, the extrapolation length λ is much smaller than the sample thickness. In this case Eq. (4) cannot be solved exactly and only an approximate value of the fundamental fluctuation wave vector can be obtained analytically. The first order correction to Eq. (5) gives for the wave vector of the fundamental mode

$$q_{z0} \simeq \frac{\pi}{d+2\lambda}. \tag{7}$$

The expression for the relaxation time of the fundamental mode [Eq. (6)] is changed accordingly and an additional term, which is proportional to the sample thickness and depends also on the extrapolation length λ, appears

$$\tau_0 = \frac{\eta}{K}\frac{d^2}{\pi^2}\left(1+\frac{4\lambda}{d}\right) \quad \text{for } \lambda \ll d. \tag{8}$$

The presence of the second term allows us to obtain the anchoring energy strength from these measurements.

In the other case, when anchoring is weak and $\lambda \gg d$, Eq. (1) and a series expansion of the secular equation yield for the relaxation time of the fundamental mode

$$\tau_0 = \frac{\eta}{2W}d\left(1+\frac{d}{6\lambda}\right), \quad \text{for } \lambda \gg d. \tag{9}$$

For small sample thicknesses the second term in the brackets is small compared to the first one and can, therefore, be neglected, leaving a linear dependence of τ on the sample thickness. This is in contrast to strong anchoring, where the dependence is quadratic in the leading term. The prefactor in Eq. (9) is inversely proportional to the anchoring energy coefficient and by measuring τ_0 as a function of sample thickness, W can be obtained. In the intermediate regime where none of the upper expansions [Eqs. (8) and (9)] is valid, the whole secular equation [Eq. (4)] has to be taken into account.

When performing the dynamic light scattering experiment, the autocorrelation function of the scattered light is detected. The fundamental mode gives the dominant contribution to the scattered light at small scattering vectors and in very thin samples [43]. For larger scattering angles and thicker samples, however, the contribution of higher fluctuation modes is significant and should not be neglected. The relaxation times $\tau_m(d)$ of the symmetric modes, which are the only ones contributing to the light scattering spectrum are obtained from different branches of the secular equation [Eq. (4)]. The relative intensity I_m of the light scattered by the mth fluctuation mode is [43]

$$I_m \propto \left(\frac{\sin\left(\frac{q_{zm}-q_s}{2}d\right)}{\left(\frac{q_{zm}-q_s}{2}d\right)}\right)^2 \frac{d^2}{q_{zm}^2}, \tag{10}$$

where q_{zm} is the z component of the mth mode wave vector and q_s is the magnitude of the scattering vector, assumed to be parallel to the z axis.

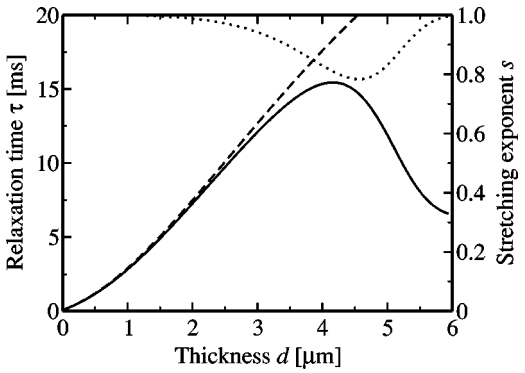

FIG. 1. Numerically calculated relaxation time τ as a function of sample thickness d plotted as a solid line. The extrapolation length is $\lambda_\varphi = 200$ nm, the scattering vector is $q = 1.5\ \mu\text{m}^{-1}$ and the first three modes are taken into account. The dashed line represents the relaxation time of the fundamental mode only. The dotted line is the numerically obtained stretching exponent s as a function of sample thickness d.

In order to study the influence of higher fluctuation modes on the average relaxation time observed in light scattering experiment, we simulate the measured autocorrelation function. As the modes are statistically independent, the observed $g^{(2)}$ is the sum over all modes, weighted by I_m. The resulting autocorrelation function is well described by the stretched exponential decay [44]

$$g^{(2)}(t) = A + Be^{-(t/\tau)^s}, \tag{11}$$

with two relevant fitting parameters: an effective relaxation time τ, and stretching exponent s. For thin samples and small scattering angles, when only one mode is observed, $s=1$ and $\tau=\tau_0$. Each deviation from this value of s indicates either nonnegligible contributions of other fluctuation modes, or a disoriented sample [45]. The value of s can, therefore, be considered also a figure of merit for the quality and reliability of each measurement.

The calculated effective relaxation time associated with $g^{(2)}$ with several contributing modes is plotted as a function of sample thickness in Fig. 1 (solid line), whereas the dashed line represents the relaxation time of the fundamental mode. The extrapolation length used in the calculation was $\lambda_\varphi = 200$ nm and the scattering vector was $q = 1.5\ \mu\text{m}^{-1}$. As one can observe, the deviation in the effective relaxation time from the relaxation time of the fundamental mode becomes apparent for sample thicknesses larger than $d \sim 2\ \mu$m. In thicker parts of the sample higher modes prevail, τ reaches a maximum value at $d \approx 4\ \mu$m, and then decreases with increasing thickness. This is because the main contribution to the relaxation time comes from higher fluctuation modes with the wave vector that matches most the scattering wave vector. As these modes have larger relaxation rates than the fundamental mode, the relaxation time is decreased. The stretching exponent s was also obtained from the numerical calculations and is shown in Fig. 1 as a dotted line. In the thin region where the fundamental mode prevails, s equals 1. In thicker samples, where higher modes appear, s is reduced, whereas in the region where the contribution of

the first mode becomes negligible, s increases again as the light scattered by the next fluctuation mode is dominant.

III. DYNAMIC LIGHT SCATTERING EXPERIMENT

The dynamic light scattering (DLS) experiment was performed with a standard photon correlation setup with a He-Ne laser operating at 632.8 nm. The normalized intensity autocorrelation function [35]

$$g^{(2)}(t)=\frac{\langle I(t')I(t'+t)\rangle}{\langle I(t')\rangle^2}, \tag{12}$$

with I being the intensity of the detected light, was measured using the ALV-5000 correlator. The selection of scattering geometry and the polarizations of the incoming and outgoing beams allowed us to observe one specific fluctuation mode and to determine the corresponding anchoring energy coefficient. In both cases (azimuthal and zenithal anchoring) the scattering angles were fairly small (up to a few degrees) so that the scattering length was large compared to the sample thickness and that as few modes as possible were observed, preferably only the fundamental mode.

A. Preparation of the samples

The liquid crystal used in our experiment was 4-*n*-pentyl-4′-cyanobiphenyl (5CB) from Sigma-Aldrich and used as received without further purification. The aligning substrates were rubbed nylon and photoactive poly-(vinyl-cinnamate) (PVCi) [46,47] coatings. In order to achieve different anchoring regimes, nylon was rubbed three times for the measurements of moderately strong anchoring (sample A), four times for very strong anchoring (sample B), whereas to achieve weak anchoring, the PVCi was used (sample C). This sample was prepared with the glass plates dipped into the solution of PVCi in chloroform, dried, and illuminated with linearly polarized UV light in order to induce anisotropy in the alignment substrate. The procedure of preparation of this sample is in detail described elsewhere [15]. Glass plates with treated surfaces were then used to prepare wedge cells by inserting spacers between the glass plates only on one side. To achieve very small sample thickness in the thin part of the cell, the glass plates had to be clearly cut and firmly pressed together. The thickness of wedge cells was accurately determined by interferometric method using a spectrophotometer and the obtained thickness was varying from 200 nm to 6 μm. Easy axes on both plates in the cell were parallel, giving a homogeneous liquid crystal alignment. The cells were filled with liquid crystal in the nematic phase with the flow direction parallel to the substrate easy axes. During the measurements the temperature was kept constant at 32 °C, i.e., 3.5 K below the nematic-isotropic transition temperature $T_{NI}=35.5\,^{\circ}\mathrm{C}$.

B. Azimuthal anchoring energy measurement

In order to determine the azimuthal anchoring energy coefficient the twist fluctuations in a nematic slab had to be observed. This was achieved by the DLS setup shown in Fig. 2(a): the polarization of the incoming light $\vec{i}$ was perpendicular to the scattering plane and the outgoing beam polarization $\vec{f}$ lay in the plane. The orientation of the nematic director $\mathbf{n_0}$ was parallel to the incoming polarization and to the direction of the sample thickness gradient. The scattering angle θ was constant during the experiment and was chosen between 2°–3°, which minimized the contribution of bend fluctuations and, therefore, an almost pure twist mode was observed. The chosen setup enabled us to measure the relaxation time of the fundamental twist mode as a function of sample thickness by simply moving the sample in the direction perpendicular to the scattering plane.

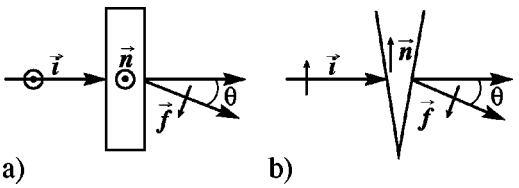

FIG. 2. Experimental setup for the measurements of the anchoring energy coefficients. (a) The polarization of the incoming beam $\vec{i}$ is parallel to the director $\mathbf{n_0}$ but perpendicular to the scattering plane and the polarization of the outgoing beam $\vec{f}$. This setup enables us to measure the azimuthal anchoring coefficient. (b) Zenithal anchoring is measured when both polarizations and director lie in the scattering plane. Scattering angle in both cases is fairly small (up to a few degrees).

An example of measured autocorrelation curve from which the relaxation time τ at a given thickness d was derived is shown in Fig. 3, where circles represent the measured data. The data can be well fitted with stretched exponential decay function [Eq. (11)], shown as a solid line. The coefficient B in Eq. (11) is determined by the intensity of the dynamically scattered light. In our case $B\ll 1$, which means that the measurement was performed in a strong heterodyne regime and that the characteristic decay time τ indeed equals the fluctuation relaxation time [35].

C. Zenithal anchoring energy coefficient

The zenithal anchoring coefficient was measured by observing the splay fluctuations in the planar nematic sample,

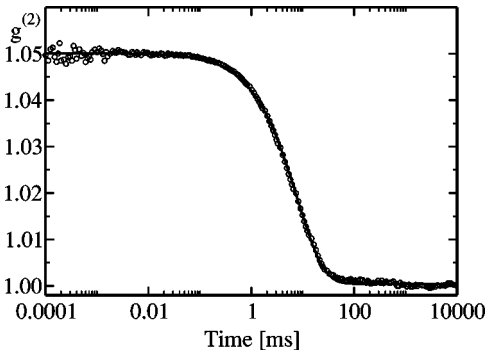

FIG. 3. Measured autocorrelation function of dynamically scattered light on nematic 5CB. The circles represent the measured data, the solid line is stretched exponential fit to the data with the parameters: $A=1.000\pm0.001$, $B=0.0496\pm0.0005$, $\tau_r=(7.86\pm0.05)$ ms, and $s=0.84\pm0.03$.

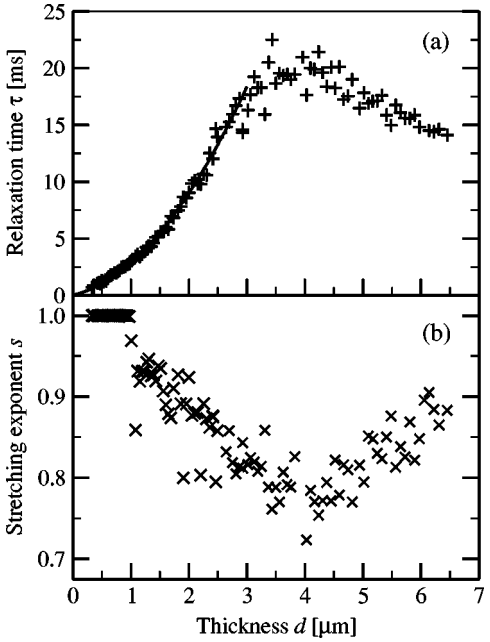

FIG. 4. Measured fluctuation relaxation time τ (a) and stretching exponent s (b) as a function of sample thickness d for sample A. The crosses are the measured data, the solid line is the parabolic fit to the data at small sample thicknesses. Deviation becomes significant for thicknesses larger than $\approx 3\ \mu$m.

which was only possible with the arrangement shown in Fig. 2(b). Polarizations of the incoming and outgoing beams lay in the scattering plane and so did the director. As both polarizations were parallel, the main contribution to the detected beam was the statically scattered light by the glass plates and only a small fraction of the detected light was dynamically scattered by fluctuations in the liquid crystal. The fitted coefficient B [Eq. (11)] is thus very small, of the order of 10^{-4}, which is approximately 100 times smaller than in the measurements of azimuthal anchoring. The autocorrelation function, therefore, had to be measured for a considerably longer time in order to obtain sufficient signal.

IV. RESULTS AND DISCUSSION

The measurements were performed on cells with three different substrates in order to study the fluctuation dynamics and to determine the anchoring energy coefficients in three different anchoring regimes. Using the moderately rubbed nylon (sample A), the autocorrelation functions of the scattered light were measured in a wide range of sample thicknesses, extending from ~ 300 nm to $\sim 6.5\ \mu$m. The decay of the autocorrelation functions was analyzed in terms of the stretched exponential function [Eq. (11)] and two parameters were obtained as a function of the sample thickness: the effective relaxation time τ and the stretching exponent s, as shown in Fig. 4. In the thinner part of the sample, up to $\sim 3\ \mu$m, the parabolic dependence of the relaxation time τ on the sample thickness is observed, implying that a pure fundamental mode was detected and that the surface anchoring was fairly strong. Fitting the parabolic expansion [Eq. (8)] to the experimental data in this region yields $\lambda_\varphi = (200 \pm 10)$ nm and the corresponding anchoring energy coefficient is $W_\varphi = (1.4 \pm 0.2) \times 10^{-5}$ J/m^2. The other parameter obtained from this fit is the ratio of the Frank elastic constant to the effective rotational viscosity. At 32 °C, the fitted value $K_2/\eta = (6.4 \pm 0.4) \times 10^{-11}$ m^2/s is in excellent agreement with the data for 5CB found in the literature [48–51]. Also, consistency of this fitting parameter implies the reliability of the obtained extrapolation length.

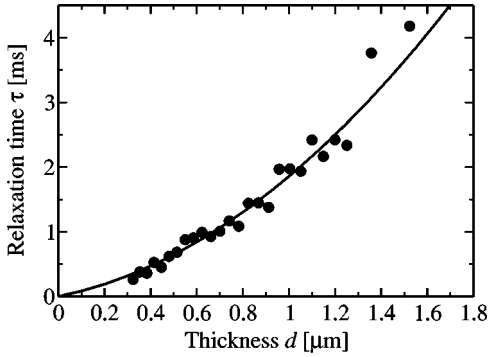

FIG. 5. Relaxation time τ of the splay fluctuations as a function of sample thickness for 5CB on moderately rubbed nylon (sample A). The zenithal extrapolation length is determined from the parabolic fit and the obtained value is $\lambda_\vartheta = (150 \pm 40)$ nm.

For thicknesses above $\approx 3\ \mu$m the relaxation time ceases to increase, reaches a maximum at $\sim 4\ \mu$m and then slowly decreases with increasing thickness towards the bulk value. This indicates that the contributions of higher fluctuation modes are not negligible in this range, which is consistent with the calculated dependence of $\tau(d)$ (Fig. 1). Apart from the relaxation times, also the stretching exponent s was obtained from this experiment and the results are shown in Fig. 4(b). Its behavior is in good agreement with the predictions of the numerical calculations (Fig. 1): for small thicknesses, s equals 1, meaning that pure fundamental twist mode was indeed observed, and then decreases to the lowest value of 0.75. This minimum is achieved at the same thickness where τ reaches its maximum value. Above $\sim 4\ \mu$m s again increases. This is because the next higher mode prevails and the contribution of the first mode becomes less important. In conclusion, we may say that the azimuthal anchoring energy coefficient can only be determined by observing the dynamic light scattering at small sample thicknesses, where the pure fundamental mode is detected. This means that the measurements should be performed at thicknesses below $\sim 2\ \mu$m, depending on the anchoring strength, the viscoelastic constants of the liquid crystal, and on the scattering length, which was in our case $\approx 4\ \mu$m.

In order to measure the zenithal anchoring energy coefficient using the same sample, the fundamental splay fluctuation mode has to be observed. The measured dependence of the relaxation time τ is plotted as a function of d in Fig. 5. The dependence of the splay mode relaxation time on the sample thickness is parabolic, indicating strong anchoring regime. Using the same procedure as in the case of strong azimuthal anchoring, zenithal extrapolation length $\lambda_\vartheta = (150 \pm 40)$ nm is obtained from the fit independently of the viscoelastic constants. This value corresponds to the an-

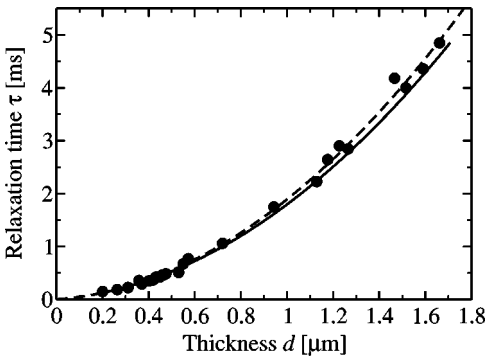

FIG. 6. Measured fluctuation relaxation time as a function of sample thickness for strong azimuthal anchoring (sample *B*). Circles represent the measured data, solid line the parabolic fit, and the dashed line the fit of the whole secular equation. The obtained extrapolation length is $\lambda_\varphi=(50\pm8)$ nm.

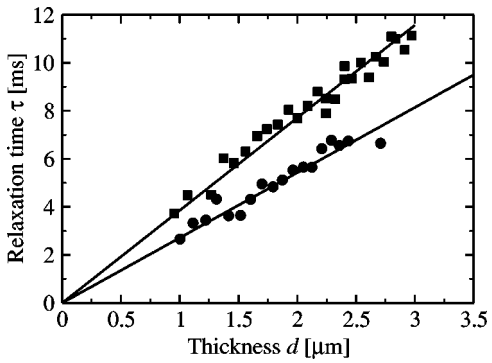

FIG. 7. Relaxation times of the twist (squares) and splay (circles) fluctuation modes as a function of sample thickness for 5CB on photoactive PVCi (sample *C*). The linear fit yields $W_\varphi=(5.3\pm0.3)\times10^{-6}$ J/m^2 and $W_\vartheta=(9.1\pm0.85)\times10^{-6}$ J/m^2.

choring energy coefficient $W_\vartheta=(2.9\pm1.0)\times10^{-5}$ J/m^2. The second fitting parameter yields the ratio $K_1/\eta=(8.9\pm2.5)\times10^{-11}$ m^2/s, which is slightly less, but consistent with the data found in the literature [48–51].

A comparison between the two obtained anchoring energy coefficients, $W_\varphi=(1.4\pm0.2)\times10^{-5}$ J/m^2 and $W_\vartheta=(2.9\pm1.0)\times10^{-5}$ J/m^2, can now be made. We find that the zenithal anchoring is stronger than the azimuthal, but only by a factor of 2. This is in contrast to what was reported earlier [23], where one or even two orders of magnitude difference between the coefficients was observed. However, as the dynamic light scattering method enables us to determine both coefficients on the same sample using the same method, we believe that the present comparison between the two anchoring coefficients is more reliable.

The measurements of the anchoring energy coefficients on sample *B*, where a very strong anchoring was expected because of additional rubbing of the aligning layer, were performed for thickness ranging from 0.2 to 2 μm. In this region, only the fundamental mode was observed ($s=1$) and the obtained relaxation time is plotted as a function of sample thickness in Fig. 6, where the circles represent the measurements and the solid line the best fit of Eq. (8) to the experimental data. The obtained azimuthal extrapolation length for strongly rubbed nylon is four times smaller than in the previous case, i.e., $\lambda_\varphi=(50\pm10)$ nm. This value corresponds to the anchoring energy coefficient of $W_\varphi=(5.6\pm1.2)\times10^{-5}$ J/m^2. The other parameter obtained from this fit is the ratio of the viscoelastic constants that depends only on the LC properties and should be the same as when measuring the anchoring coefficient on moderately rubbed sample. At 32 °C, the fitted value $K_2/\eta=(6.84\pm0.3)\times10^{-11}$ m^2/s is in excellent agreement with the previously obtained value. The dashed line in Fig. 6 is obtained by fitting the whole secular equation [Eq. (4)] to the measured data. Also in this case, λ_φ can be derived directly without knowing the viscoelastic constants of the liquid crystal. The obtained value $\lambda_\varphi=(50\pm8)$ nm matches exactly the one obtained from the parabolic fit, confirming that for strong anchoring the parabolic expansion yields reliable and accurate values of the anchoring energy coefficient.

The zenithal anchoring energy coefficient was also determined on the strongly rubbed nylon sample (sample *B*). However, due to the fact that for a reliable analysis, the extrapolation length should not be much smaller than the thickness of the thinnest part of the cell, the extrapolation length in this case could not be accurately determined. The obtained values $\lambda_\vartheta=(37\pm30)$ nm and $W_\vartheta=(1.2\pm0.9)\times10^{-4}$ J/m^2 are thus merely estimates.

The third set of measurements was performed in a sample where weak anchoring was expected. Using the photoaligned sample (sample *C*), the obtained fluctuation relaxation time as a function of sample thickness is shown in Fig. 7. The squares represent the relaxation times of the twist fluctuation mode, from which the azimuthal anchoring strength was determined, and the circles represent the splay relaxation times used to determine the zenithal anchoring energy coefficient. In both cases the dependence is linear; according to Eq. (9) this means that the anchoring of liquid crystal on the photoalignment layer is weak. The anchoring coefficients are then obtained by fitting Eq. (9) to the experimental data. The azimuthal anchoring energy coefficient is found to be $W_\varphi=(5.3\pm0.3)\times10^{-6}$ J/m^2 and the zenithal $W_\vartheta=(9.1\pm0.85)\times10^{-6}$ J/m^2. We, therefore, observe that also in the case of weak anchoring induced on photosensitive alignment layer, the two anchoring energy coefficients differ less than by a factor of 2. It should be noted that linear dependence of the relaxation time on the sample thickness extends up to $d\sim3$ μm, indicating that the contributions of the higher fluctuation modes are negligible.

V. CONCLUSIONS

In this paper we have shown that the dynamic light scattering experiment is suitable for measurements of not only azimuthal but also of zenithal anchoring energy coefficient using the same planar nematic liquid crystal sample. In contrast to previously used methods, where external torques were applied to the liquid crystal during the measurement, the present method is based on the observation of intrinsic thermal fluctuations and does not affect the uniform configuration. Using a wedge cell, we confirmed experimentally that the relaxation time of the fundamental fluctuation mode de-

pends linearly on the sample thickness in the case of weak anchoring and parabolically in the case of strong anchoring. We found that the linear and quadratic expansions for the relaxation time are valid only to a certain thickness, beyond which the fundamental mode is overcome by higher fluctuation modes and the measured relaxation time changes drastically. Therefore the measurement of the anchoring energy coefficient of 5CB on different substrates should be performed at sample thicknesses below ~ 3 μm. The azimuthal anchoring coefficient depends strongly on the sample preparation and on the treatment of the alignment layers. In our experiment the zenithal anchoring energy coefficient was measured on the same sample and under the same external conditions as the azimuthal coefficient. Using differently rubbed nylon and photoactive PVCi, we found that the ratio of the two anchoring energy coefficients is $W_\vartheta / W_\varphi \simeq 2$ for all anchoring regimes and substrates used in our experiment.

[1] J. A. Castelano, Mol. Cryst. Liq. Cryst. **94**, 33 (1983).
[2] J.-H. Kim and Ch. Rosenblatt, J. Appl. Phys. **84**, 6027 (1998).
[3] B. S. Ban and Y. B. Kim, J. Phys. Chem. B **103**, 3869 (1999).
[4] Y.-M. Zhu *et al.*, Appl. Phys. Lett. **65**, 49 (1994).
[5] Y. B. Kim *et al.*, Appl. Phys. Lett. **66**, 2218 (1995).
[6] H. Nejoh, Surf. Sci. **256**, 94 (1991).
[7] M. F. Toney *et al.*, Nature (London) **374**, 709 (1995).
[8] S.-C. Hong *et al.*, Phys. Rev. E **63**, 051706 (2001).
[9] X. Wei *et al.*, Phys. Rev. Lett. **82**, 4256 (1999).
[10] J. M. Geary, J. W. Goodby, A. R. Kmetz, and J. S. Patel, J. Appl. Phys. **62**, 4100 (1987).
[11] J. L. Janning, Appl. Phys. Lett. **21**, 173 (1972).
[12] W. M. Gibbons, P. J. Shannon, S.-T. Sun, and B. J. Swetlin, Nature (London) **351**, 49 (1991).
[13] M. O'Neill and S. M. Kelly, J. Phys. D **33**, R67 (2000).
[14] S. Perny *et al.*, Liq. Cryst. **27**, 329 (2000).
[15] M. Vilfan, I. Drevenšek Olenik, A. Mertelj, and M. Čopič, Phys. Rev. E **63**, 061709 (2001).
[16] M. Murata *et al.*, Jpn. J. Appl. Phys., Part 2 **31**, L189 (1992).
[17] N. Kawatsuki *et al.*, Macromolecules **30**, 6680 (1997).
[18] S. D. Evans *et al.*, J. Phys. Chem. B **101**, 2143 (1997).
[19] M. Ruetschi, P. Grutter, J. Funfschilling, and H. J. Gunterodt, Science **265**, 512 (1994).
[20] P. Chaudhari *et al.*, Nature (London) **411**, 56 (2001).
[21] B. Jérôme, Rep. Prog. Phys. **54**, 391 (1991).
[22] G. Barbero and G. Durand, in *Liquid Crystals in Complex Geometries*, edited by G. P. Crawford and S. Žumer (Taylor & Francis, London, 1996), Chap. 2.
[23] B. Jérôme, in *Handbook of Liquid Crystals*, edited by D. Demus, J. Goodby, G. W. Gray, H.-W. Spiess, and V. Vill (Wiley, New York, 1998), Vol. 1, p. 535, and references within.
[24] Y. Iimura, N. Kobayashi, and S. Kobayashi, Jpn. J. Appl. Phys., Part 2 **33**, L434 (1994).
[25] V. P. Vorflusev, H.-S. Kitzerow, and V. G. Chigrinov, Jpn. J. Appl. Phys., Part 2 **34**, L1137 (1995).
[26] E. Pollosat and I. Dozov, Mol. Cryst. Liq. Cryst. Sci. Technol., Sect. A **282**, 223 (1996).
[27] H. Yokoyama and H. A. van Sprang, J. Appl. Phys. **57**, 4520 (1985).
[28] D.-F. Gu, S. Uran, and Ch. Rosenblatt, Liq. Cryst. **19**, 427 (1995).
[29] F. Yang, J. R. Sambles, and G. W. Bradberry, J. Appl. Phys. **85**, 728 (1999).
[30] Y. A. Nastishin, R. D. Polak, S. V. Shiyanovskii, V. H. Bodnar, and O. D. Lavrentovich, J. Appl. Phys. **86**, 4199 (1999).
[31] S. Naemura, Appl. Phys. Lett. **33**, 1 (1978).
[32] K. H. Yang and Ch. Rosenblatt, Appl. Phys. Lett. **43**, 62 (1983).
[33] S. Faetti and M. Nobili, Liq. Cryst. **25**, 487 (1998).
[34] G. Barbero and G. Durand, Mol. Cryst. Liq. Cryst. **203**, 33 (1991).
[35] B. J. Berne and R. Pecora, *Dynamic Light Scattering* (Wiley, New York, 1976).
[36] Orsay Group on Liquid Crystals, Phys. Rev. Lett. **22**, 1361 (1969); J. Chem. Phys. **51**, 816 (1969).
[37] I. Haller and J. D. Litster, Phys. Rev. Lett. **25**, 1550 (1970); Mol. Cryst. Liq. Cryst. **12**, 277 (1971).
[38] M. M. Wittebrood, Th. Rasing, S. Stallinga, and I. Muševič, Phys. Rev. Lett. **80**, 1232 (1998).
[39] M. Vilfan and M. Čopič, Mol. Cryst. Liq. Cryst. Sci. Technol., Sect. A **351**, 419 (2000).
[40] P. G. de Gennes and J. Prost, *The Physics of Liquid Crystals* (Clarendon, Oxford, 1993).
[41] S. Stallinga, M. M. Wittebrood, D. H. Luijendijk, and Th. Rasing, Phys. Rev. E **53**, 6085 (1996).
[42] A. Mertelj and M. Čopič, Phys. Rev. E **61**, 1622 (2000).
[43] A. Mertelj and M. Čopič, Mol. Cryst. Liq. Cryst. Sci. Technol., Sect. A **320**, 287 (1998).
[44] C. P. Lindsey and G. D. Patterson, J. Chem. Phys. **73**, 3348 (1980).
[45] A. Mertelj and M. Čopič, Mol. Cryst. Liq. Cryst. Sci. Technol., Sect. A **282**, 35 (1996).
[46] P. L. Egerton, E. Pitts, and A. Reiser, Macromolecules **14**, 95 (1981).
[47] M. Schadt, K. Schmitt, V. Kozinkov, and V. Chigrinov, Jpn. J. Appl. Phys., Part 1 **31**, 2155 (1992).
[48] J.-i. Hirakata *et al.*, Jpn. J. Appl. Phys., Part 2 **25**, L607 (1986).
[49] D. Gu *et al.*, Macromolecules **24**, 2385 (1991).
[50] G.-P. Chen, H. Takezoe, and A. Fukuda, Liq. Cryst. **5**, 341 (1989).
[51] R. Borsali, D.Y. Yoon, and R. Pecora, J. Phys. Chem. B **102**, 6337 (1998).